Two-photon resonant multiphoton ionization and stimulated emission in krypton and xenon

John C. Miller
Chemical Physics Section, Health and Safety Research Division, Oak Ridge National Laboratory, P.O. Box 2008, Oak Ridge, Tennessee 37831-6125
(Received 19 June 1989)

Forward- and backward-directed, stimulated emissions have been observed following two-photon pumping of the $5p$ states of krypton and the $6p'$, $7p$, $8p$, and $4f$ states of xenon. Multiphoton ionization spectra are also obtained and compared with the photon-detected excitation spectra. In krypton coherent emissions from the $5p$ states to the $5s$ are observed, and for xenon many $p \rightarrow s$, $d \rightarrow p$, and $f \rightarrow d$ cascade emissions are observed. By analogy to the well-studied alkali-metal and alkaline-earth examples, the emissions are assigned as amplified spontaneous emission. Several intensity anomalies in the xenon $p \rightarrow s$ emissions are not understood at present. Interference effects due to coherent cancellation between competing excitation pathways may be occurring.

INTRODUCTION

Ever since the first report in 1967 of the production of coherent vacuum-ultraviolet radiation via third-harmonic generation (THG) in rare gases, techniques for increasing its efficiency have been explored.[1] The utility of two-photon resonance enhancement of the nonlinear susceptibility was recognized very early for metal-vapor systems.[2,3] Along with the increased efficiency of THG, however, came the observation that a panoply of competing nonlinear processes also became important when exciting at, or near, two-photon resonance. These can include multiphoton ionization (MPI), stimulated electronic Raman scattering (SERS), stimulated hyper-Raman scattering (SHRS), amplified spontaneous emission (ASE), and parametric four-wave mixing (PFWM). Furthermore, these new emissions present in the laser focus can also interact with the pump radiation to generate new coherent waves by other four-wave- or six-wave-mixing schemes. These processes have been studied in detail for the alkali metal, alkaline earth, and group IIB metals which have relatively low-lying two-photon allowed absorptions and large nonlinear susceptibilities. Several comprehensive reviews[2,3] and a recent paper[4] provide references to, and details of, most of the prior studies. Although parasitic to conversion to the ultraviolet, SERS, in particular, is a major source of coherent tunable infrared (ir) radiation. Very high conversion efficiencies have been reported in some cases.[5]

In contrast to metal vapors, only a few brief studies of these processes in rare gases have appeared[6-8] in spite of their usefulness for vacuum-ultraviolet generation via THG. This is because the lowest two-photon resonances occur in the ultraviolet where intense, tunable laser light has only recently become readily available. Furthermore, the expected coherent emissions range from the vuv to the far infrared making detection difficult.

Multiphoton ionization (MPI) has proven to be an important adjunct to optical detection in the study of nonlinear optical processes. For a number of years we have been investigating nonlinear processes in dense rare gases. In particular, we have used both ionization and direct optical detection to characterize THG and MPI and their mutual interactions.[9-15]

In the present work, we continue these studies with the use of ultraviolet lasers capable of accessing two-photon resonances in krypton and xenon. We cannot detect the THG directly because its wavelength is too short to be transmitted by window materials. However, the nonlinear absorption can be investigated via MPI or the detection of visible or infrared photons from amplified stimulated emission. The two-photon resonant, third-harmonic generation has, however, been observed in supersonic jets.[16,17]

APPARATUS

The required wavelengths are generated by frequency doubling the beam from a pulsed dye laser (Lambda Physik, EMG101, FL2000E) in a crystal of β-barium borate (BBO) cut at 65° (CSK Lmt). The crystal is angle tuned, either by hand or with a feedback-controlled system (Inrad), to produce excitation spectra. The generated ultraviolet light of wavelength 212–228 nm ($\sim$1 mJ) is separated in a Pellin-Broca prism and then loosely focused by a 50-cm quartz lens into a MPI cell with Suprasil windows. The cell is of standard design, with a central wire collector and cylindrical outer electrode. Guard electrodes prevent electrons formed at the windows from reaching the interaction region. The electron signal is amplified and displayed on an oscilloscope. For recording excitation spectra a boxcar integrater is used to average the signal. Upon exiting the cell, the forward-directed light is recollimated and focused into an appropriate monochromater-detector combination. For the visible and near-infrared light an optical multichannel analyzer is used. For higher resolution a $1\frac{1}{4}$-m monochromator and photomultiplier tube are available. Searches in the vuv or ir were carried out with an evacuated spectrometer (Macpherson) and solar-blind photo-

tube or a $\frac{1}{4}$-m monochromator and photodiode, respectively. For backward-generated emissions the laser was reflected into the MPI cell by an uv dichroic mirror (266 nm) such that the backward visible or ir light was transmitted and redirected into the detection system. Wavelength calibration was provided by krypton and xenon penlights (Oriel) which emitted many of the same wavelengths as observed in the laser-exited gas. Finally, lifetimes were measured with a fast ir photodiode whose output was averaged in a digital oscilloscope.

RESULTS

Krypton

The tuning range possible with the present BBO doubling crystal encompasses several two-photon-allowed resonances in krypton. Excitation at 216.6, 214.7, or 212.6 nm excites the $5p[5/2]_2$, $5p[3/2]_2$, and $5p[1/2]_0$ states, respectively. The latter excitation, which falls near the high-energy limit of the doubling crystal, was considerably weaker and not extensively studied. Figure 1 shows a schematic energy-level diagram for krypton which illustrates the excitations and emissions relevant to the present study. The notation $nl[K]_J$ conforms to that used in Charlotte Moore's tables[18] and reflects j-l coupling. In this scheme, n and l designate the principal quantum number and orbital angular momentum, respectively, of the orbital into which the electron is promoted, K gives the total angular momentum of the core plus the orbital angular momentum of the promoted electron, and J is the total angular momentum. These two-photon resonances (especially the $5p[5/2]_2$) have previously been used to enhance the nonlinear susceptibility, and hence the conversion efficiency for third-harmonic generation[16,17] and sum- and difference-frequency mixing[19,20] in krypton. In addition, using an intense tunable ArF laser near 193 nm Shahidi *et al.*[21] have excited the higher energy $6p[3/2]_2$ level and observed several stimulated emissions including ASE, SHRS, and PFWM. Only the latter study, which employed very high peak power picosecond pulses (10^{11}–10^{12} W/cm^2), reported such processes.

In the present study both MPI and stimulated emissions have been observed following two-photon excitation. Figure 2 shows an excitation spectrum for the (2+1) MPI of krypton at 425 Torr showing the $5p[3/2]_2$ and $5p[5/2]_2$ resonances. The observed width of 0.13 Å for the $5p[3/2]_2$ transition reflects the laser bandwidth although the slightly wider $5p[5/2]$ line implicates an additional broadening mechanism which will be discussed later. No other resonances were observed and no dimer effects were noted over the pressure range from 1–500 Torr.

Upon tuning the laser to each of the resonances, intense forward- and backward-directed near-infrared light was observed with the optical multichannel analyzer. Figure 3 shows an emission spectrum (forward direction) following excitation of the $5p[5/2]_2$ state. The emissions were observed only when tuned exactly (within the laser linewidth) to resonance, and the excitation spectrum was identical to that of the MPI spectrum of Fig. 2. Using the high-resolution monochrometer, each emission wavelength was determined to be identical (±0.01 nm) to that of a Kr resonance lamp although a factor of 2–3 broader. Using a fast photodiode, the time profile of the emission at low pressure was the same as that of the laser, ~8 ns full width at half maximum (FWHM), as shown in Fig. 4. The normal fluorescence lifetimes are 20–40 ns according to both theoretical[22] and experimental results.[23] The branching ratios of the emissions are also approximately

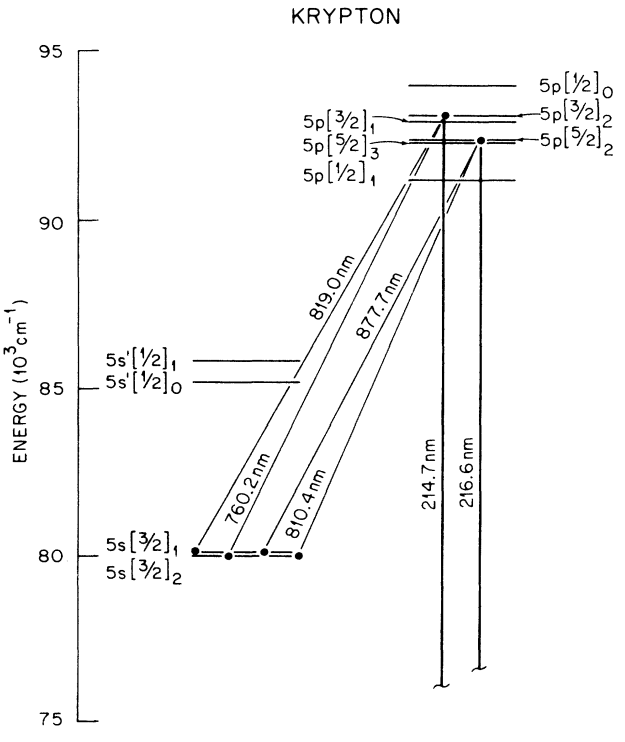

FIG. 1. Schematic energy-level diagram for krypton showing excitation wavelengths and those for observed emissions.

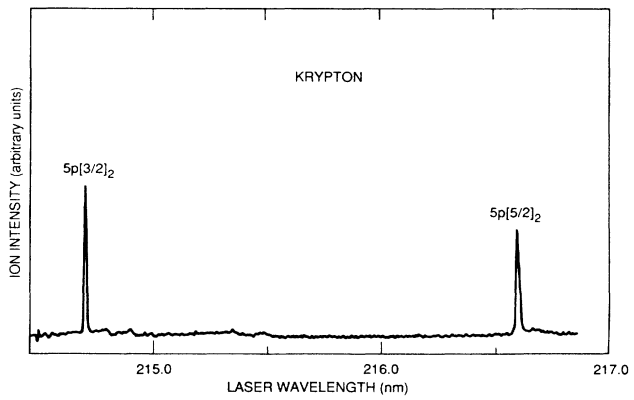

FIG. 2. Excitation spectrum for the (2+1) MPI of krypton.

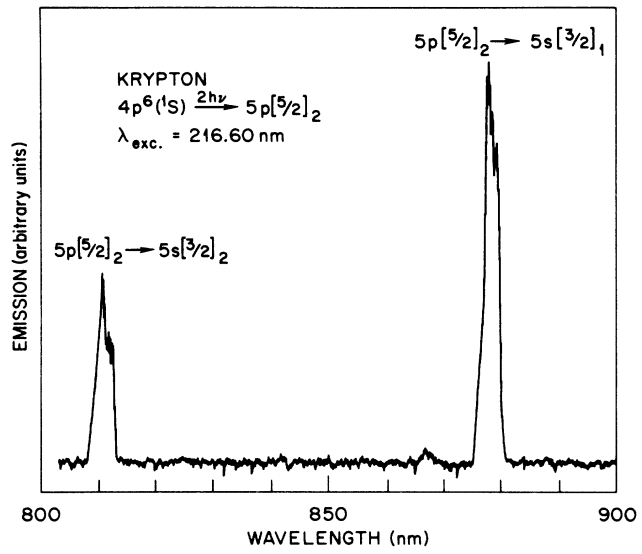

FIG. 3. Forward-directed emission spectrum of krypton following excitation of the $5p[5/2]_2$ state.

in accord with theory[22] and experiment.[23] Finally, the emissions were polarized parallel to the input laser for $\Delta J=1$ transitions and perpendicular for $\Delta J=0$ transitions as expected from selection rules. The corresponding emissions to the $5s'[1/2]_0$ and $5s'[1/2]_1$ levels would occur in the 1.21–1.55-μm region and could not be observed with the present apparatus.

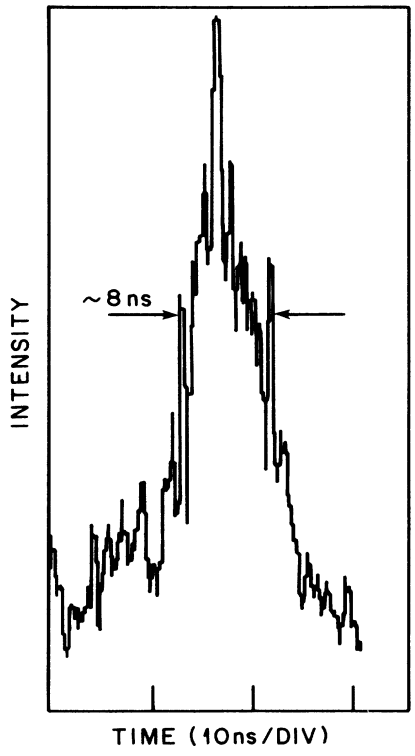

FIG. 4. Time profile of the emission of Fig. 3 detected with a fast photodiode.

All of the above measurements are consistent with assignment of the emissions as amplified spontaneous emission (ASE) which is sometimes referred to as optically pumped stimulated emission. Strong pumping of the $5p$ levels creates a population inversion relative to the $5s$ and $5s'$ levels. Fluorescence emitted along the laser beam in either the forward or reverse direction is then amplified by stimulated emissions from the inverted population. The stimulated nature of the observed emissions is obvious from the intensity (visible ASE from xenon can be observed by the eye in a darkened room), bidirectionality, divergence (similar to the input laser), and short lifetime. It is quite striking that the ASE can be readily detected over a meter from the cell with no additional recollimation or focusing. Since the laser bandwidth is larger than the intrinsic width of the $5p$ levels, any SHRS, which is an off-resonant process, could not be distinguished from the resonantly produced ASE.

Finally, when the laser is tuned in the red wing of the $5p[5/2]_2$ transition, an additional weak emission is observed at 811.3 nm which can be assigned as ASE originating from the $5p[5/2]_3$ state and terminating on the $5s[3/2]_2$ state. The $5p[5/2]_3$ and $5p[5/2]_2$ states are only separated by 13 cm^{-1} which corresponds to a splitting of only 0.03 nm in the spectrum of Fig. 2. Although not resolved, excitation to this state may be contributing to the extra linewidth mentioned previously. Excitation of $J=3$ states with two photons is forbidden in the dipole approximation but may occur via a two-photon quadrupole ($E2$-$E2$) mechanism. Gornick *et al.*[24] have previously reported two-photon excitation of the $5d[5/2]_3$ and $5d[7/2]_3$ states in xenon and attributed them to $E1$-$E2$- or $E2$-$E1$-type transitions. However, the nearest quadrupole-allowed transitions, which could serve as intermediate states, are off resonant by more than 26 000 cm^{-1}. The same is true for the present case. At pressures of 50–100 Torr, however, collisional intermultiplet mixing may be producing the population in the $J=3$ state. Higher-resolution studies are required in order to distinguish these possibilities.

Xenon

For xenon, the accessible tuning range overlaps the two-photon wavelengths required for excitation of the $6p'$, $7p$, $8p$, and $4f$ manifolds. Figure 5 shows the relative energies of these levels as well as a summary of the observed emissions to be discussed later. The third-photon ionization is also shown. No results on these resonances have previously appeared although several groups have extensively studied two-photon excitation of the lower energy $6p$ and $5d$ states.[24,25] A few brief reports of ASE (Refs. 25 and 26) and even lasing[6] following these excitations have appeared. As was the case for krypton, these same resonances have been used to enhance the efficiency of THG (Refs. 16 and 17) or FWM.[27,28]

Figure 6 shows the MPI spectra in the spectral region of the $6p'$ and $7p$ states at high pressure (100 Torr). These spectra are broader than the laser linewidth and clearly show dimer effects as asymetric broadening or

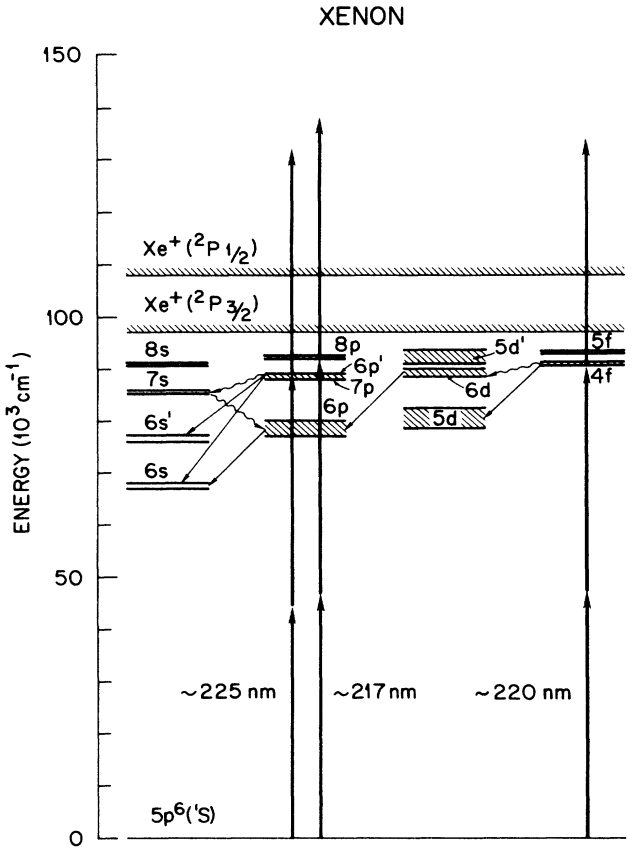

FIG. 5. Schematic energy-level diagram for xenon showing excitation, ionization, and emission pathways. Straight arrows represent observed pathways. Wavy lines indicate emissions which were not detected but can be inferred as described in the text.

even additional bands. In contrast, MPI spectra at 20 Torr show no such distinct features although they are still broader than the laser linewidth. Because of the high pressure and temperature and the low vibrational frequencies of Xe_2, no structured spectra are expected. The spectra of the dimers of Kr_2, Xe_2, and various mixed dimers have, however, been very nicely studied in these spectral regions by resonantly enhanced MPI in supersonic jet expansions.[29] The dimer features observed in Fig. 6 are very similar to those seen in previous studies of dense xenon near the $6p$ states by Gornik *et al.*[24] and Keto and co-workers.[25] In particular, Raymond *et al.*[25] have extensively modeled the line shapes and extracted the potential curves of the dimers associated with the $6p$ levels. The red "humps" associated with each peak are interpreted as satellites arising from extrema in the difference potential. The new peaks observed between the atomic lines may then be due to transitions of bound dimers. Due to the limited resolution in the present experiments such detailed analysis is not warranted; however, the same qualitative arguments apply.

Figure 5 also shows a summary of the observed emissions following the two-photon excitations. The straight arrows indicate emissions between the various manifolds which are directly observed. The wavy arrows indicate nonobserved emissions (generally in the far ir) which were not detected with the present apparatus but which may be inferred from the presence of the observed "cascade" emissions.

As a specific example, Fig. 7 shows a detailed energy-level diagram for the case of two-photon excitation at 224.29 nm to the $6p'[3/2]_2$ state. Note that for clarity only the even J levels (i.e., two-photon allowed from the ground state) of the $6p', 7p$ manifold are shown in the figure. Once excited, a population inversion exists relative to all lower levels except the ground state and ASE is

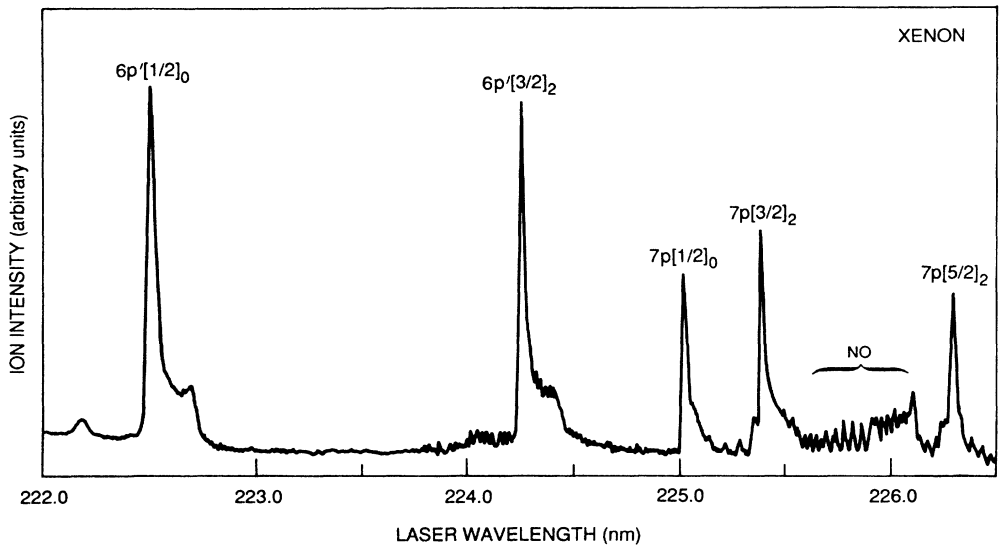

FIG. 6. The MPI spectrum of xenon in the region of the $6p'$ and $7p$ states at 100 Torr. A very small amount of nitric oxide impurity gives rise to the rotationally resolved structure near 226 nm.

expected whenever permitted by selection rules and with intensities mediated by dipole matrix elements. Thus, from the initially excited $6p'[3/2]_2$ level, ASE to both $7s$ levels is expected (the $6p'[3/2]_2 \rightarrow 7s[3/2]_1$ transition should be considerably weaker[21]) and presumably does occur as evidenced by cascade $6p$-$6s$ emission. However, the 2.52- and 2.68-μm emissions could not be observed with our detector. Of the $6s'$ final states only the $6p'[3/2]_2 \rightarrow 6s'[1/2]_1$ transition is allowed, and the emission at 834.7 nm is observed strongly in both the forward and backward directions. Both emissions to the $6s$ state are dipole allowed and published branching ratios, α, for emission to the $6s[3/2]_1$ and $6s[3/2]_2$ states, respectively, are similar from both theory ($\alpha = 1.4$) and fluorescence experiments ($\alpha = 2.8$). However, in the present work only the $6p'[3/2]_2 \rightarrow 6s[3/2]_2$ transition at 452.5 nm is observed. This emission can be seen by the eye in a darkened room after filtering the excitation light. The corresponding emission to the $6s[3/2]_1$ state at 473.4 nm is just barely observable in the forward direction after recollimating the emissions and using large slits for detection. The observed ratio is thus approximately $\alpha \leq 0.016$ in marked contrast to the above-cited values which are greater than 1. In the reverse direction only the 452.4-nm emission is observed, and the signal-to-noise ratio gives an upper limit to the ratio of $\alpha \sim 0.1$. Similarly, when the $7p[3/2]_2$ state is initially excited, ASE to the $6s[3/2]_2$ state is readily observed but that to the corresponding $J = 1$ level is absent. Again, the theoretical and flourescence branching ratios of 5.8 and 3.9, respectively, are nearly equal to 1. We will return to this point later.

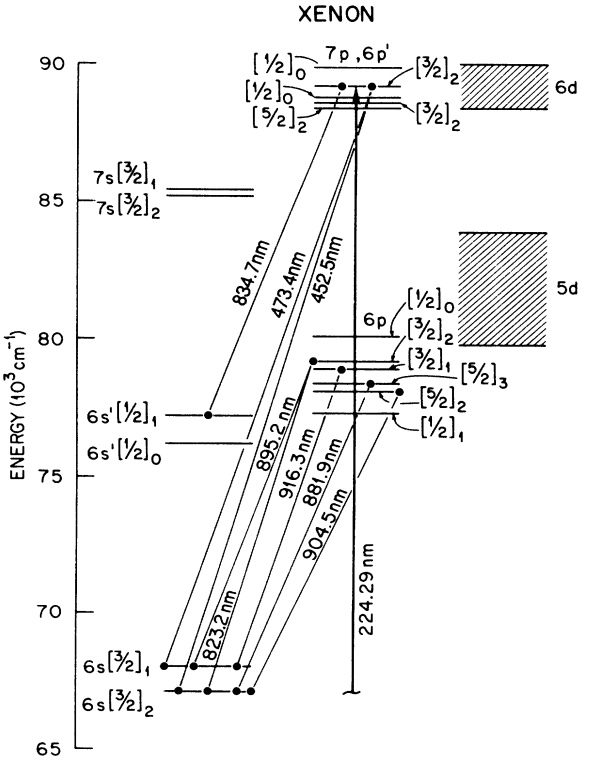

FIG. 7. Coherent emissions observed from xenon following two-photon excitation of the $6p'[3/2]_2$ state.

ASE to the $6d$ and $5d$ manifolds is expected but not observed due to our limited ir detection capability. Again, the observed $6p$-$6s$ cascade emission suggests that these states may be relay states (intermediate states between the initially pumped state and the upper level of some other observed emission). Of the d states the $6p'[3/2]_2 \rightarrow 6d[3/2]_2$ and $\rightarrow 5d[1/2]_1$ transitions are significantly more probable than all other possibilities.[21]

Five emissions connecting the $6p$ and $6s$ manifolds are observed. Because $6p$ states are populated via $7s$, $6d$, or $5d$ relay states, their initial populations should reflect the products of the dipole matrix elements of each two-step decay summed over all possible decay routes. The relative intensities of the cascade $6p \rightarrow 6s$ emissions would then include the $6p$ relative population factors as well as the $6p$-$6s$ coupling matrix elements. In general, within factors of five or so, the intensities of the observed lines are in accord with these arguments, using line strength factors from Aymar and Coulombe.[22] Of the possible emissions three lie outside of our detection limits. Another transition, $6p[3/2]_1 \rightarrow 6s[3/2]_2$, has a line strength factor an order of magnitude less than the weakest observed emission. Finally, the $6p[1/2]_2 \rightarrow 6s[3/2]_1$ transition is not observed even though it has a reasonable line strength. However, it *is* observed following two-photon excitation of the $6p'[1/2]_0$ level. For $6p'[3/2]_2$ excitation, however, the population transfer to the $6p[1/2]$ level must be the limiting factor, and this conclusion is easily rationalized. As mentioned, the most probable relay states for excitation of the $6p$ manifolds are the $7s[3/2]_2$, the $6d[3/2]_2$, and the $5d[1/2]_1$ states. Of these, only the latter can connect to the $6p[1/2]_0$ by dipole selection rules, but this level actually lies at a lower energy than the $6p[1/2]_0$ state by 132 cm^{-1}. The next most probable relay state is the $6d[1/2]_1$, which has only moderate coupling strength with the $6p[1/2]_0$. However, when the initial excitation is to the $6p'[1/2]_0$ state both the $7s[3/2]_1$ and $6d[3/2]_1$ states provide suitable relay states with strong coupling to both the $6p'[1/2]_0$ and $6p[1/2]_0$ levels.

In the same manner, following excitation of each of the allowed two-photon $6p'$ and $7p$ states, a number of both direct and cascade emissions are observed and are listed in Table I. Generally the relative intensities can be rationalized as in the last paragraph by a qualitative consideration of selection rules and oscillator strengths. One interesting observation deserves additional note. Excitation of the $6p'[1/2]_0$ level results in weak emission on the $6p[5/2]_3 \rightarrow 6s[3/2]_2$ line at 881.9 nm. No scheme involving a single relay state can account for the $\Delta J = 3$ transition. A more tortuous route involving three relay states must be invoked as follows:

$$6p'[1/2]_0 \rightarrow 6d[3/2]_1 \rightarrow 7p[3/2]_1 \rightarrow 5d[5/2]_2 \rightarrow 6p[5/2]_3 .$$

Although more complicated, each of the steps has a moderate or high oscillator strength. Alternately the

weak emission could result from collisional cascade processes rather than radiative ones.

Finally, excitation of the $4f$ and $8p$ states results in a more limited number of emissions which are listed in Table I. Again, in general, the observed emissions can be rationalized in a rather straightforward manner.

Remaining to be discussed is the large disparity between the p-s branching ratios from fluorescence experiments and from theory, as compared to those observed in the forward direction in the present experiments. The present result is that the ASE from the $6p'[3/2]_2$ and $7p[3/2]_2$ to the $6s[3/2]_1$ state is either missing or unex-

TABLE I. Observed coherent emissions and assignments following two-photon absorption in krypton and xenon.

Excitation		Emission	
λ (nm, air)	Assignment	λ (nm, air)	Assignment
Krypton			
216.60	$5p[5/2]_2$	810.4	$5p[5/2]_2 \rightarrow 5s[3/2]^0_2$
		877.7	$5p[5/2]_2 \rightarrow 5s[3/2]^0_1$
216.60	$5p[5/2]_3$	811.3	$5p[5/2]_3 \rightarrow 5s[3/2]^0_2$
214.70	$5p[3/2]_2$	760.2	$5p[3/2]_2 \rightarrow 5s[3/2]^0_2$
		819.0	$5p[3/2]_2 \rightarrow 5s[3/2]^0_1$
212.49	$5p[1/2]_0$	(not studied)	
Xenon			
226.30	$7p[5/2]_2$	881.9	$6p[5/2]_3 \rightarrow 6s[3/2]^0_2$
225.44	$7p[3/2]_2$	462.4	$7p[3/2]_2 \rightarrow 6s[3/2]^0_2$
		823.2	$6p[3/2]_2 \rightarrow 6s[3/2]^0_2$
		840.9	$6p[3/2]_1 \rightarrow 6s[3/2]^0_2$
		881.9	$6p[5/2]_3 \rightarrow 6s[3/2]^0_2$
		895.2	$6p[3/2]_2 \rightarrow 6s[3/2]^0_1$
		904.5	$6p[5/2]_2 \rightarrow 6s[3/2]^0_2$
		916.3	$6p[3/2]_1 \rightarrow 6s[3/2]^0_1$
225.05	$7p[1/2]_0$	840.9	$6p[3/2]_1 \rightarrow 6s[3/2]^0_2$
		904.5	$6p[5/2]_2 \rightarrow 6s[3/2]^0_2$
		916.3	$6p[3/2]_1 \rightarrow 6s[3/2]^0_1$
224.24	$6p'[3/2]_2$	452.5	$6p'[3/2]_2 \rightarrow 6s[3/2]^0_2$
		473.4	$6p'[3/2]_2 \rightarrow 6s[3/2]^0_1$
		834.7	$6p'[3/2]_2 \rightarrow 6s'[1/2]^0_1$
		823.2	$6p[3/2]_2 \rightarrow 6s[3/2]^0_2$
		881.9	$6p[5/2]_3 \rightarrow 6s[3/2]^0_2$
		895.2	$6p[3/2]_2 \rightarrow 6s[3/2]^0_1$
		904.5	$6p[5/2]_2 \rightarrow 6s[3/2]^0_2$
222.50	$6p'[1/2]_0$	458.3	$6p'[1/2]_0 \rightarrow 6s[3/2]^0_1$
		788.7	$6p'[1/2]_0 \rightarrow 6s'[1/2]^0_1$
		823.2	$6p[3/2]_2 \rightarrow 6s[3/2]^0_2$
		828.0	$6p[1/2]_0 \rightarrow 6s[3/2]^0_1$
		840.9	$6p[3/2]_1 \rightarrow 6s[3/2]^0_2$
		881.9	$6p[5/2]_3 \rightarrow 6s[3/2]^0_2$
		895.2	$6p[3/2]_2 \rightarrow 6s[3/2]^0_1$
		904.5	$6p[5/2]_2 \rightarrow 6s[3/2]^0_2$
		916.3	$6p[3/2]_1 \rightarrow 6s[3/2]^0_1$
220.07[a]	$4f[3/2]_2$	920.3	$4f[3/2]_2 \rightarrow 5d[1/2]^0_1$
		949.7	$4f[3/2]_2 \rightarrow 5d[3/2]^0_2$
		873.9	$6d[3/2]^0_2 \rightarrow 6p[1/2]_1$
		886.2	$6d[1/2]^0_1 \rightarrow 6p[1/2]_1$
		895.2	$6p[3/2]_2 \rightarrow 6s[3/2]^0_1$
219.93[a]	$4f[5/2]_2$	944.2	$4f[5/2]_2 \rightarrow 5d[3/2]^0_2$
		886.2	$6d[1/2]^0_1 \rightarrow 6p[1/2]_1$
		898.8	$6d[5/2]^0_2 \rightarrow 6p[5/2]_2$
		904.5	$6p[5/2]_2 \rightarrow 6s[3/2]^0_2$
		916.3	$6p[3/2]_1 \rightarrow 6s[3/2]^0_1$
216.80[a]	$8p[5/2]_2$	881.9	$6p[5/2]_3 \rightarrow 6s[3/2]^0_2$
216.45[a]	$8p[3/2]_2$	881.9	$6p[5/2]_3 \rightarrow 6s[3/2]^0_2$
216.02[a]	$8p[1/2]_0$	881.9	$6p[5/2]_3 \rightarrow 6s[3/2]^0_2$

[a]The $4f$ and $8p$ levels were less thoroughly investigated and only the strongest emissions were observed.

pectedly weak while that to the corresponding $J=2$ level is readily observed, even by the eye. If we remember that the $6s[3/2]_1$ state can optically couple to the ground state, then a four-wave mixing process of the form $\omega_3(\text{vuv})=2\omega_1(\text{exc})-\omega_2(p\rightarrow s)$ might be anticipated. Subsequently, the direct (ω_3) and indirect ($2\omega_1-\omega_2$) excitation pathways to the $6s[3/2]_1$ level could interfere destructively in such a way as to inhibit the $p\rightarrow s$ amplified spontaneous emission. This is essentially the interference effect first proposed by Manykin and Afanas'ev[30] and experimentally studied by Boyd and collaborators[31] and Garrett *et al.*[32] Attempts were made to directly observe light at or near 146.9 nm; however, the intense scattered excitation light could only be incompletely filtered and precluded observation of weak vuv emission. Further experiments are required in order to investigate the possibility of this type of interference.

CONCLUSIONS

Following strong two-photon pumping of the $5p$ states of krypton and the $6p'$, $7p$, $4f$, and $8p$ levels of xenon, we have characterized both the (2+1) MPI and the ASE that results. Although a few limited reports have appeared previously, the present results represent the first comprehensive study of these processes in rare gases. These results have important implications in other areas of laser–rare-gas interactions. In particular, both ASE and MPI are parasitic to any two-photon resonant four-wave mixing.[2,3] In addition to saturation effects due to strong two-photon excitation, the generated emissions may be strong enough to cause ac Stark shifting of the initially pumped level, thus reducing the resonance effect. Furthermore, the ground-state depletion and subsequent population redistribution will change both the nonlinear susceptibility as well as the phase-matching conditions. In the same way, MPI will cause population redistribution but, in addition, the resulting plasma may cause Stark broadening. MPI has even been implicated in the normally forbidden second-harmonic generation in gases. Finally, the generated ASE may further combine with the pump radiation to give other parametric processes. Although not observed here, such processes are well known for metal systems[5] and have been observed by Shahidi *et al.*[21] for krypton.

The redistribution of populations is also an important consideration in kinetic studies of high-pressure gases which model rare gas and rare-gas halide excimer lasers. Finally, several very recent studies[33–35] in flames and plasmas have detected atomic carbon and atomic oxygen by observing the forward-directed ASE following two-photon excitation. These authors have suggested the analytical utility of such a diagnostic technique.

ACKNOWLEDGMENTS

Research sponsored by the Office of Health and Environmental Research, U.S. Department of Energy under Contract No. DE-AC05-84OR21400 with Martin Marietta Energy Systems, Inc. Several useful discussions with M. G. Payne and W. R. Garrett are also gratefully acknowledged.

[1] G. H. C. New and J. F. Ward, Phys. Rev. Lett. **19**, 556 (1967).
[2] J. J. Wynne and P. P. Sorokin, in *Nonlinear Infrared Generation,* edited by Y. R. Shen (Springer-Verlag, Berlin, 1977), pp. 159–214.
[3] C. R. Vidal, in *Tunable Lasers,* edited by L. F. Mollenauer and J. C. White (Springer-Verlag, Berlin, 1987), pp. 56–113.
[4] B. K. Clark, M. Masters, and J. Huennekens, Appl. Phys. B **47**, 159 (1988).
[5] S. M. Hamadani, J. A. D. Stockdale, R. N. Compton, and M. S. Pindzola, Phys. Rev. A **34**, 1938 (1986).
[6] A. W. McCown, M. N. Ediger, and J. G. Eden, Phys. Rev. A **26**, 2281 (1982).
[7] V. A. Kartazaev, Opt. Spektrosk. **62**, 714 (1987) [Opt. Spectrosc. (USSR) **62**, 425 (1987)].
[8] M. B. Rankin, J. P. Davis, C. Giranda, and L. C. Bobb, Opt. Commun. **70**, 345 (1989).
[9] J. C. Miller, R. N. Compton, M. G. Payne, and W. R. Garrett, Phys. Rev. Lett. **45**, 114 (1980).
[10] J. C. Miller and R. N. Compton, Phys. Rev. A **25**, 2056 (1982).
[11] R. N. Compton and J. C. Miller, J. Opt. Soc. B **2**, 355 (1985).
[12] W. R. Garrett, W. R. Ferrell, M. G. Payne, and J. C. Miller, Phys. Rev. A **34**, 1165 (1986).
[13] P. R. Blazewicz, M. G. Payne, W. R. Garrett, and J. C. Miller, Phys. Rev. A **34**, 5171 (1986).
[14] P. R. Blazewicz, J. A. D. Stockdale, J. C. Miller, T. Efthimiopoulos, and C. Fotakis, Phys. Rev. A **35**, 1092 (1987).
[15] P. R. Blazewicz and J. C. Miller, Phys. Rev. A **38**, 2863 (1988).
[16] R. H. Page, R. J. Larkin, A. H. Kung, Y. R. Shen, and Y. T. Lee, Rev. Sci. Instrum. **58**, 1616 (1987), and references therein.
[17] K. Miyazaki, H. Sakai, and T. Sato, Appl. Opt. **28**, 699 (1989).
[18] C. E. Moore, *Atomic Energy Levels,* Natl. Bur. Stand. (U.S.) Circ. No. 467 (U.S. GPO, Washington, D.C., 1952), Vol. III.
[19] K. D. Bonin and T. J. McIlrath, J. Opt. Soc. Am. B **2**, 527 (1985).
[20] G. Hilber, A. Lago, and R. Wallenstein, J. Opt. Soc. Am. B **4**, 1753 (1987).
[21] M. Shahidi, T. S. Luk, and C. K. Rhodes, J. Opt. Soc. Am. B **5**, 2386 (1988).
[22] M. Aymar and M. Coulombe, Atom. Data Nucl. Data Tables **21**, 537 (1978).
[23] R. S. F. Chang, H. Horiguchi, and D. W. Setser, J. Chem. Phys. **73**, 778 (1980).
[24] W. Gornick, S. Kindt, E. Matthias, H. Rinneberg, and D. Schmidt, Phys. Rev. Lett. **45**, 1941 (1986); W. Gornick, S. Kindt, E. Matthias, and D. Schmidt, J. Chem. Phys. **75**, 68 (1981); W. Gornik, E. Matthias, and D. Schmidt, J. Phys. B **15**, 3413 (1982).
[25] N. Böwering, M. R. Bruce, and J. W. Keto, J. Chem. Phys. **84**, 709 (1986); **84**, 715 (1986); N. Böwering, T. D. Raymond, and J. W. Keto, Phys. Rev. Lett. **52**, 1880 (1984); T. D. Raymond, N. Bowering, C. Y. Kuo, and J. W. Keto, Phys. Rev. A **29**, 721 (1984).

[26]V. A. Kartazaev, Opt. Spektrosk. **62**, 714 (1987) [Opt. Spectrosc. (USSR) **62**, 425 (1987)].
[27]R. Hilbig and R. Wallenstein, IEEE J. Quantum Electron. **QE-19**, 194 (1983).
[28]S. D. Kramer, C. H. Chen, M. G. Payne, G. S. Hurst, and B. E. Lehman, Appl. Opt. **22**, 3271 (1983).
[29]P. M. Dehmer and S. T. Pratt, J. Chem. Phys. **88**, 4139 (1988), and references therein.
[30]E. A. Manykin and A. M. Afanas'ev, Zh. Eksp. Teor. Fiz. **48**, 931 (1965) [Sov. Phys.—JETP **21**, 619 (1965)]; **52**, 1246 (1967) [Sov. Phys.—JETP **25**, 828 (1967)].
[31]M. S. Malcuit, D. J. Gauthier, and R. W. Boyd, Phys. Rev. Lett. **55**, 1086 (1985).
[32]W. R. Garrett, M. A. Moore, R. K. Wunderlich, and M. G. Payne, in *Resonance Ionization Spectroscopy,* IOP Conf. Proc. Ser. No. 94, edited by T. B. Lucatorto and J. E. Parks (IOP, Bristol, 1989), p. 33.
[33]M. Aldén, U. Westblom, and J. E. M. Goldsmith, Optics Lett. **14**, 305 (1989).
[34]H. Bergström, H. Hallstadius, H. Lundberg, and A. Persson, Chem. Phys. Lett. **145**, 27 (1989).
[35]M. Aldén, P.-E. Bengtsson, and U. Westblom, Optics Commun. **71**, 263 (1989).